

# Full quantum state reconstruction of symmetric two-mode squeezed thermal states via spectral homodyne detection

Simone Cialdi,<sup>1,2</sup> Carmen Porto,<sup>1</sup> Daniele Cipriani,<sup>1</sup> Stefano Olivares,<sup>1,2</sup> and Matteo G. A. Paris<sup>1,2</sup>

<sup>1</sup>*Dipartimento di Fisica, Università degli Studi di Milano, I-20133 Milano, Italy*

<sup>2</sup>*Istituto Nazionale di Fisica Nucleare, Sezione di Milano, Via Celoria 16, I-20133 Milan, Italy*

(Dated: May 29, 2022)

We suggest and demonstrate a scheme to reconstruct the symmetric two-mode squeezed thermal states of spectral sideband modes from an optical parametric oscillator. The method is based on a single homodyne detector and active stabilization of the cavity. The measurement scheme have been successfully tested on different two-mode squeezed thermal states, ranging from uncorrelated coherent states to entangled states.

PACS numbers: 03.65.Wj, 42.50.Lc, 42.50.Dv

**Introduction** – Homodyne detection (HD) is an effective tool to characterize the quantum state of light in either the time [1–8] or the frequency [9–28] domain. In a spectral homodyne detector, the signal under investigation interferes at a balanced beam splitter with a local oscillator (LO) with frequency  $\omega_0$ . The two outputs undergo a photodetection process and their photocurrents are combined leading to a photocurrent continuously varying in time. The information about the spectral field modes at frequencies  $\omega_0 \pm \Omega$  (sidebands) is then retrieved by electronically mixing the photocurrent with a reference signal with frequency  $\Omega$  and phase  $\Psi$ . Upon varying the phase  $\theta$  of the LO, we may access different field quadratures, whereas the phase  $\Psi$  can be adjusted to select the symmetric  $\mathcal{S}$  or antisymmetric  $\mathcal{A}$  balanced combinations of the upper and lower sideband modes.

Measuring the sole modes  $\mathcal{S}$  and  $\mathcal{A}$  through homodyne detection is not enough to assess the spectral correlation between the modes under investigation [1] and, in turn, to fully characterize a generic quantum state. In order to retrieve the full information about the sidebands it has been suggested that one should spatially separate the two modes [30, 31] or implement more sophisticated setups [1, 32] involving resonator detection. On the other hand, it would be desirable to have schemes, which do not require structural modifications of the experimental setup. In turn, this would make possible to embed more easily diagnostic tools in interferometry [33] and continuous-variable-based quantum technology. Remarkably, in the relevant cases of interest for continuous variable quantum information, such as squeezed state generation by spontaneous parametric down-conversion, the correlation between the modes vanishes, due to symmetric nature of the generated state.

In this Letter we suggest and demonstrate a measurement scheme where the relevant information for the quantum state reconstruction of symmetric spectral modes is obtained by using a single homodyne detector with active stabilization through the Pound-Drever-Hall (PDH) technique [3]. In particular, the reconstruction is achieved by exploiting the phase coherence of the setup, guaranteed in every step of the experiment, and two aux-

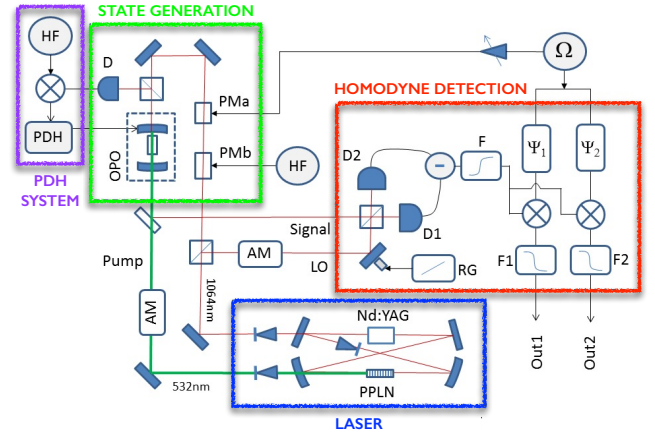


FIG. 1: Schematic diagram of the experimental setup. See the main text for details.

iliary combinations of the sideband modes selected by setting the mixer phase at  $\Psi = \pm\pi/4$ .

**Homodyne detection and state reconstruction** – A schematic diagram of our apparatus is sketched in Fig. 1. The principal radiation source is provided by a home made Nd:YAG Laser ( $\sim 300$  mW @1064 nm and 532 nm) internally-frequency-doubled by a periodically poled MgO:LiNbO<sub>3</sub> (PPLN in Fig. 1). To obtain the single mode operation, a light diode is placed inside the laser cavity. One laser output (@532 nm) pumps the MgO:LiNbO<sub>3</sub> crystal of the optical parametric oscillator (OPO) whereas the other output (@1064 nm) is sent to a polarizing beam splitter (PBS) to generate the local oscillator (LO) and the seed for the OPO. The power of the LO ( $\sim 10$  mW) is set by an amplitude modulator (AM). Two phase modulators (PMA and PMb in Fig. 1) generate both the sidebands used as OPO coherent seeds and as active stabilization of the OPO cavity with the PDH technique [3]. For the OPO stabilization we use a frequency of 110 MHz (HF) while the frequency  $\Omega$  for the generation of the input seed is about 3 MHz. This is indeed a major effort, but it will turn out to be fundamental for the *full* reconstruction of the symmetric states addressed below. The OPO cavity is linear with a free

spectral range (FSR) of 3300 MHz, the output mirror has a reflectivity of 92% and the rear mirror of 99%. The linewidth is about 55 MHz, thus the OPO stabilization frequency HF is well above the OPO linewidth while the frequency  $\Omega$  is well inside. In order to actively control the length of the OPO cavity its rear mirror is connected to a piezo that is controlled by the signal error of the PDH apparatus.

The detector consists of a 50:50 beam splitter, two low noise detectors and a differential amplifier based on a LMH6624 operational amplifier. The interferometer visibility is about 95%. We remove the low frequency signal through a high-pass filter @500 kHz and then the signal is sent to the demodulation stage. To extract the information about the signal at frequency  $\Omega$  we use an electronic setup consisting in a phase shifter, a mixer ( $\otimes$  in Fig. 1) and a low-pass filter @300 kHz. Since, as we will see in the following, we need to measure the signal at two different orthogonal phases,  $\Psi_1$  and  $\Psi_2 = \Psi_1 + \pi/2$ , for the sake of simplicity we implemented a double electronic setup to observe at the same time the outputs (see Fig. 1). Finally, the LO phase  $\theta$  is scanned between 0 and  $2\pi$  by a piezo connected with a mirror before the beam splitter of the HD. The acquisition time is 20 ms and we collect about 100 000 points by a 2 GHz oscilloscope.

If  $a_0(\omega_0)$  is the photon annihilation operator of the signal mode at the input of the HD, it is easy to show that the “fast term”  $\omega_0$  is canceled by the presence of the LO at the same frequency)  $I(t) \propto a_0(t)e^{-i\theta} + a_0^\dagger(t)e^{i\theta}$  [35], where  $\theta$  is the phase difference between signal and LO and we introduced the time-dependent field operator  $a_0(t)$ , that is slowly varying with respect to the carrier at  $\omega_0$ , such that  $a_0(t) = e^{-i\omega_0 t} \int d\omega F(\omega) a_0(\omega) e^{-i\omega t} \equiv e^{-i\omega_0 t} a_0(t)$ ,  $F(\omega)$  being the apparatus spectral response function.

To retrieve the information about the sidebands at frequencies  $\omega_0 \pm \Omega$ , described by the time-dependent field operators  $\hat{a}_{\pm\Omega}(t)$ , we use electronic mixers set at the frequency  $\Omega$  with phase shift  $\Psi$  with respect to the signal, leading to the current  $I_\Omega(t, \Psi) = I(t) \cos(\Omega t + \Psi)$ . Neglecting the terms proportional to  $\exp(\pm 2i\Omega t)$  (low-pass filter), we find the following expression for operator describing the (spectral) photocurrent  $I_\Omega(t, \Psi) \propto X_\theta(t, \Psi|\Omega)$ , where  $X_\theta(t, \Psi|\Omega) = b(t, \Psi|\Omega)e^{-i\theta} + b^\dagger(t, \Psi|\Omega)e^{i\theta}$  is the quadrature operator associated with the field operator (note the dependence on the two sidebands):

$$b(t, \Psi|\Omega) = \frac{a_{+\Omega}(t)e^{i\Psi} + a_{-\Omega}(t)e^{-i\Psi}}{\sqrt{2}}. \quad (1)$$

Note that  $[b(t, \Psi|\Omega), b^\dagger(t', \Psi|\Omega)] = \chi_{(\Delta\omega)^{-1}}(|t - t'|)$ .

The interaction inside the OPO is bilinear and involves the sideband modes  $a_{\pm\Omega}$  [35]. It is described by the effective Hamiltonian  $H_\Omega \propto a_{+\Omega}^\dagger a_{-\Omega}^\dagger + \text{h.c.}$ , that is a two-mode squeezing interaction. Due to the linearity of  $H_\Omega$ , if the initial state is a coherent state or the

vacuum, the generated two-mode state  $\varrho_\Omega$  is a Gaussian state, namely, a state described by Gaussian Wigner functions and, thus, fully characterized by its covariance matrix (CM)  $\sigma_\Omega$  and first moment vector  $\mathbf{R}$  [2, 37]. It is worth noting that due to the symmetry of  $H_\Omega$ , the two-sideband state is symmetric [1] and can be written as  $\varrho_\Omega = D_2(\alpha)S_2(\xi)\nu_{+\Omega}(N)\otimes\nu_{-\Omega}(N)S_2^\dagger(\xi)D_2^\dagger(\alpha)$ , where  $D_2(\alpha) = \exp\{[\alpha(a_{+\Omega}^\dagger + a_{-\Omega}^\dagger) - \text{h.c.}]/\sqrt{2}\}$  is the symmetric displacement operator and  $S_2(\alpha) = \exp(\xi a_{+\Omega}^\dagger a_{-\Omega}^\dagger - \text{h.c.})$  the two mode squeezing operator and  $\nu_{\pm\Omega}(N)$  is the thermal state of mode  $a_{\pm\Omega}$  with  $N$  average photons [2]. The state  $\varrho_\Omega$  belongs to the so-called class of the two-mode squeezed thermal states, generated by the application of  $S_2^\dagger(\xi)D_2^\dagger(\alpha)$  to two thermal states with (in general) different energies. In order to test our experimental setup, we acted on the OPO pump and on the phase modulation to generate and characterize three classes of states: the coherent ( $\alpha \neq 0$  and  $N, \xi = 0$ ), the squeezed ( $\xi, N \neq 0$  and  $\alpha = 0$ ) and the squeezed-coherent ( $\alpha, \xi, N \neq 0$ ) two-mode sideband state. We now consider the mode operators:

$$b(t, 0|\Omega) \equiv a_s, \quad \text{and} \quad b(t, \pi/2|\Omega) \equiv a_a, \quad (2)$$

which correspond to the symmetric ( $\mathcal{S}$ ) and antisymmetric ( $\mathcal{A}$ ) combination of the sideband modes, respectively, and the corresponding quadrature operators  $q_k = X_0(t, \Psi_k|\Omega)$ ,  $p_k = X_{\pi/2}(t, \Psi_k|\Omega)$ , and  $z_k^\pm = X_{\pm\pi/4}(t, \Psi_k|\Omega)$ ,  $k = a, s$ , with  $\Psi_s = 0$  and  $\Psi_a = \pi/2$ . In the  $\mathcal{S}/\mathcal{A}$  modal basis, the first moment vector of  $\varrho_\Omega$  reads  $\mathbf{R}' = (\langle q_s \rangle, \langle p_s \rangle, \langle q_a \rangle, \langle p_a \rangle)^T$  and its  $4 \times 4$  CM can be written in the following block-matrix form:

$$\sigma' = \begin{pmatrix} \sigma_s & \sigma_\delta \\ \sigma_\delta^T & \sigma_a \end{pmatrix}, \quad \sigma_\delta = \begin{pmatrix} \epsilon_q & \delta_{qp} \\ \delta_{pq} & \epsilon_p \end{pmatrix}, \quad (3)$$

where [38]:

$$\sigma_k = \begin{pmatrix} \langle q_k^2 \rangle - \langle q_k \rangle^2 & \frac{1}{2}(\langle z_k^+ \rangle^2 - \langle z_k^- \rangle^2) \\ \frac{1}{2}(\langle z_k^+ \rangle^2 - \langle z_k^- \rangle^2) & \langle p_k^2 \rangle - \langle p_k \rangle^2 \end{pmatrix} \quad (4)$$

is the CM of the mode  $k = a, s$ ,  $\epsilon_l = \langle l_s l_a \rangle - \langle l_s \rangle \langle l_a \rangle$ ,  $\delta_{l\bar{l}} = \langle l_s \bar{l}_a \rangle - \langle l_s \rangle \langle \bar{l}_a \rangle$  with  $l, \bar{l} = q, p$  and  $l \neq \bar{l}$ . The matrix elements of  $\sigma_k$  can be directly measured from the homodyne traces of corresponding mode  $a_k$  [39], whereas the entries of  $\sigma_\delta$  cannot. However, the information about  $\epsilon_l$  can be retrieved by changing the value of the mixer phase to  $\Psi = \pm\pi/4$ . In fact, it is easy to show that [38, 40, 41]  $\epsilon_l = \frac{1}{2}(\langle l_\pm^2 \rangle - \langle l \rangle^2) - \langle l_s \rangle \langle l_a \rangle$ ,  $l = q, p$ , where  $q_\pm = X_0(t, \pm\pi/4|\Omega)$  and  $p_\pm = X_{\pi/2}(t, \pm\pi/4|\Omega)$ .

We now focus on  $\delta_{l\bar{l}}$ . Given the state  $\varrho_\Omega$ , but with different thermal contributions, these elements are equal to the energy unbalance between the sidebands (without the contribution due to the displacement that does not affect the CM) [39], namely,  $\delta_{qp} = -\delta_{pq} = \Delta N_\Omega = (N_{+\Omega} - N_{-\Omega})$ , which cannot be directly accessed by the spectral homodyne detection alone. To overcome this issue, a resonator detection method has been proposed and

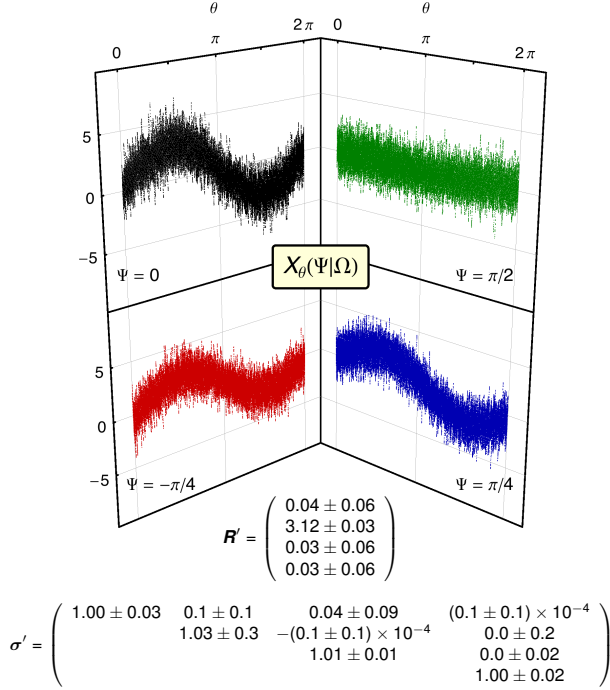


FIG. 2: Homodyne traces referring to the coherent two-mode sideband state and the reconstructed  $\mathbf{R}'$  and  $\sigma'$ . The purities of the modes  $\mathcal{S}$  and  $\mathcal{A}$  are  $\mu_s = 0.99 \pm 0.02$  and  $\mu_a = 0.99 \pm 0.01$ , respectively. Only the relevant elements are shown.

demonstrated in Refs. [1, 32]. In our case we can exploit the error signal from the PDH stabilization to check the symmetry of the sideband state and also to measure the presence of some energy unbalance of the two sidebands, leading to non-vanishing  $\delta_{ii}$ . More in details, given the cavity bandwidth, the PDH error signal allows to measure the unbalance as [39]  $\Delta N_\Omega = (\tau_{+\Omega} - \tau_{-\Omega})N_\Omega$ , where  $\tau_{\pm\Omega}$  are the relative transmission coefficients associated with the two sideband modes and  $N_\Omega = N_{+\Omega} + N_{-\Omega}$  can be obtained from the (reconstructed) diagonal elements of  $\sigma_s$  and  $\sigma_a$  [39, 42].

*Experimental results* – Given the state  $\varrho_\Omega$ , the full reconstruction of the CM requires the measurement of the quadratures of modes  $a_s, a_a$ , and  $a_\pm = b(t, \pm\pi/4|\Omega)$ . Once the mode has been selected by choosing the suitable mixer phase  $\Psi$ , the LO phase  $\theta$  was scanned from 0 to  $2\pi$  to acquire the corresponding homodyne trace. The statistical analysis of each trace allows to reconstruct the expectation value of the moments of the quadrature required to reconstruct the CM  $\sigma'$  and the first moments vector  $\mathbf{R}'$ .

Figures 2, 3 and 4 show the experimental spectral homodyne traces corresponding to the coherent, squeezed and squeezed-coherent two-mode sideband states, respectively. In the same figures we report the corresponding  $\sigma'$  and  $\mathbf{R}'$ . All the reconstructed  $\sigma'$  satisfy the physical condition  $\sigma' + i\Omega \geq 0$  where  $\Omega = i\sigma_y \oplus \sigma_y$ ,  $\sigma_y$  being the Pauli matrix [2]. This implies that the

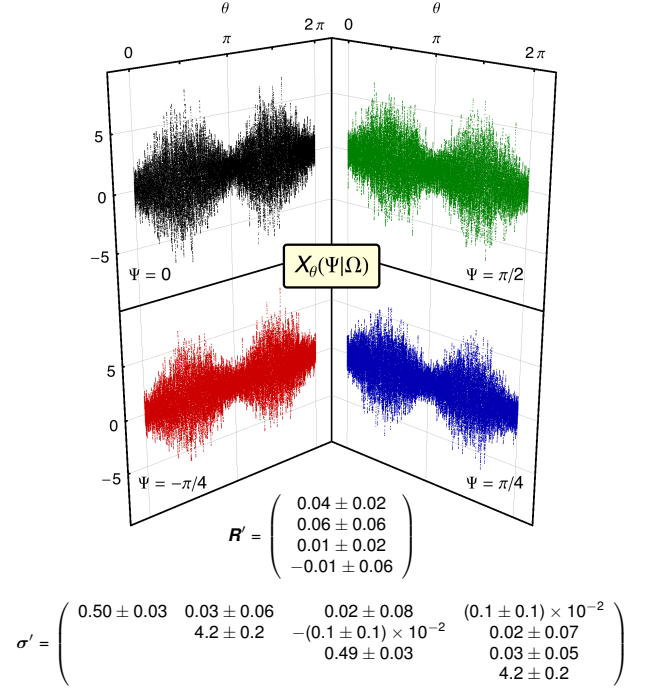


FIG. 3: Homodyne traces referring to the squeezed two-mode sideband state and the reconstructed  $\mathbf{R}'$  and  $\sigma'$ . The noise reduction is  $3.1 \pm 0.3$  dB for both the modes  $\mathcal{S}$  and  $\mathcal{A}$ , whereas their purities are  $\mu_s = 0.68 \pm 0.07$  and  $\mu_a = 0.67 \pm 0.02$ , respectively. Only the relevant elements are shown.

---

• *Two-mode coherent state:*

$$\mathbf{R} = (0.05 \pm 0.06, 2.18 \pm 0.05, 0.01 \pm 0.06, 2.23 \pm 0.05)^T$$

$$\sigma_\Omega = \begin{pmatrix} 1.00 \pm 0.02 & 0.0 \pm 0.1 & 0.00 \pm 0.02 & 0.1 \pm 0.1 \\ 0.0 \pm 0.1 & 1.02 \pm 0.02 & 0.0 \pm 0.1 & 0.01 \pm 0.02 \\ 0.00 \pm 0.02 & 0.0 \pm 0.1 & 1.00 \pm 0.02 & 0.0 \pm 0.1 \\ 0.1 \pm 0.1 & 0.01 \pm 0.02 & 0.0 \pm 0.1 & 1.02 \pm 0.02 \end{pmatrix}$$


---

• *Two-mode squeezed state:*

$$\mathbf{R} = (0.02 \pm 0.04, 0.03 \pm 0.04, 0.03 \pm 0.04, 0.05 \pm 0.04)^T$$

$$\sigma_\Omega = \begin{pmatrix} 2.3 \pm 0.1 & 0.00 \pm 0.06 & -1.8 \pm 0.1 & 0.05 \pm 0.06 \\ 0.00 \pm 0.06 & 2.3 \pm 0.1 & 0.01 \pm 0.06 & 1.8 \pm 0.1 \\ -1.8 \pm 0.1 & 0.01 \pm 0.06 & 2.3 \pm 0.1 & 0.00 \pm 0.06 \\ 0.05 \pm 0.06 & 1.8 \pm 0.1 & 0.00 \pm 0.06 & 2.3 \pm 0.1 \end{pmatrix}$$


---

• *Two-mode squeezed-coherent state:*

$$\mathbf{R} = (-0.09 \pm 0.05, 4.02 \pm 0.06, -0.03 \pm 0.05, 4.02 \pm 0.06)^T$$

$$\sigma_\Omega = \begin{pmatrix} 2.4 \pm 0.1 & 0.1 \pm 0.2 & -1.8 \pm 0.1 & 0.0 \pm 0.2 \\ 0.1 \pm 0.2 & 2.3 \pm 0.1 & -0.2 \pm 0.2 & 1.8 \pm 0.1 \\ -1.8 \pm 0.1 & -0.2 \pm 0.2 & 2.4 \pm 0.1 & -0.1 \pm 0.2 \\ 0.0 \pm 0.2 & 1.8 \pm 0.1 & -0.1 \pm 0.2 & 2.3 \pm 0.1 \end{pmatrix}$$


---

TABLE I: Reconstructed first moment vectors  $\mathbf{R}$  and CMs  $\sigma_\Omega$  of the two-mode sideband states  $\varrho_\Omega$  corresponding to the states of Figs. 2, 3 and 4, respectively.

modes  $\mathcal{S}$  and  $\mathcal{A}$  represent the same local quantum state,

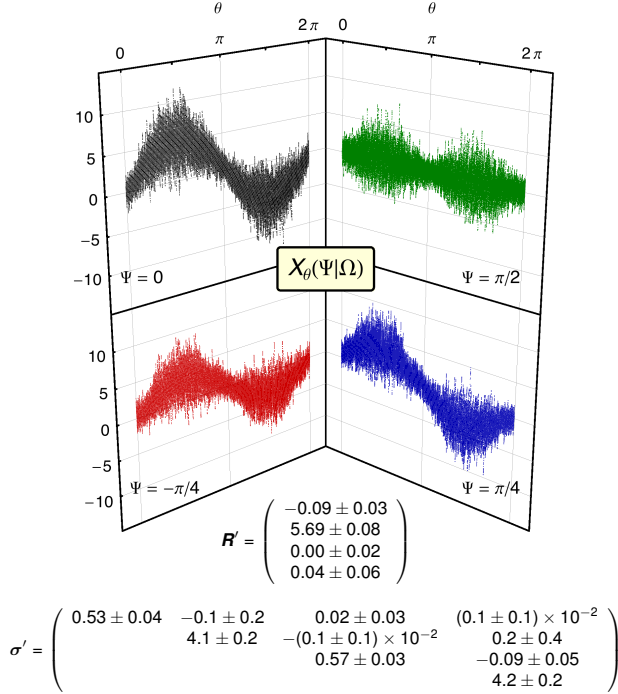


FIG. 4: Homodyne traces referring to the squeezed-coherent two-mode sideband state and the reconstructed  $\mathbf{R}'$  and  $\boldsymbol{\sigma}'$ . The noise reduction is  $2.7 \pm 0.3$  dB for the  $\mathcal{S}$  mode and  $2.4 \pm 0.2$  dB for the  $\mathcal{S}$  mode, whereas the purities are  $\mu_s = 0.68 \pm 0.07$  and  $\mu_a = 0.64 \pm 0.02$ , respectively. Only the relevant elements are shown.

namely,  $\boldsymbol{\sigma}_s = \boldsymbol{\sigma}_a$ : this is in agreement with our measurement within statistical errors, as one can check from the Figs. 2, 3 and 4. Furthermore, the diagonal elements of the off-diagonal blocks are zero within their statistical errors, in agreement with the expectation for a factorized state of the two modes.

We should now calculate the corresponding CMs in the modal basis  $\hat{a}_{+\Omega}$  and  $\hat{a}_{-\Omega}$  of the upper and lower sideband, respectively. Because of Eqs. (2) we can write  $\boldsymbol{\sigma}_\Omega = \mathbf{S}^T \boldsymbol{\sigma}' \mathbf{S}$  and  $\mathbf{R} = \mathbf{S}^T \mathbf{R}'$ , where

$$\mathbf{S} = \frac{1}{\sqrt{2}} \begin{pmatrix} \mathbb{I} & \mathbb{I} \\ -i\boldsymbol{\sigma}_y & i\boldsymbol{\sigma}_y \end{pmatrix} \quad (5)$$

is the symplectic transformation associated with the

mode transformations of Eqs. (2). The results are summarized in Table I. Whereas the reconstructed two-mode sideband coherent state is indeed a product of two coherent states, the other two reconstructed states exhibit non-classical features. In particular, the minimum symplectic eigenvalues of the corresponding partially transposed CMs [43, 44] read  $\tilde{\lambda} = 0.50 \pm 0.02$  and  $\tilde{\lambda} = 0.55 \pm 0.03$  for the two-mode squeezed and squeezed-coherent state, respectively: since in both the cases  $\tilde{\lambda} < 1$ , we conclude that the sideband modes are entangled.

*Concluding remarks* – In conclusion, we have presented a measurement scheme to fully reconstruct the class of symmetric two-mode squeezed thermal states of spectral sideband modes, a class of states with Gaussian Wigner functions widely exploited in continuous variable quantum technology. The scheme is based on a homodyne detection and active stabilization, which guarantees phase coherence in every step of the experiment, and on a suitable analysis of the detected photocurrents. We have shown that by properly choosing the electronic mixer phase it is possible to select four different combinations of the upper and lower sideband which, together with the information from the PDH error signal, allows to reconstruct the elements of the covariance matrix of the state under consideration. The scheme has been successfully demonstrated to reconstruct both factorized and entangled sideband states.

In our implementation we have used two electronic mixers and retrieved information about two modes at a time. It is also possible to use four mixers and extract information about the four modes at the same time. The method is based on a single homodyne detector and does not involve elements outside the main detection tools of continuous variable optical systems. As such, our procedure is indeed a versatile diagnostic tool, suitable to be embedded in quantum information experiments with continuous variable systems in the spectral domain.

*Acknowledgments* – This work has been supported by UniMI through the UNIMI14 grant 15-6-3008000-609 and the H2020 Transition Grant 15-6-3008000-625, and by EU through the collaborative project QuProCS (Grant Agreement 641277). MGAP and SO thank Alberto Porzio for useful discussions.

[1] A. I. Lvovsky, H. Hansen, T. Aichele, O. Benson, J. Mlynek, and S. Schiller, Phys. Rev. Lett. **87**, 050402 (2001).  
[2] A. Zavatta, M. Bellini, P. L. Ramazza, F. Marin, and F. T. Arecchi, J. Opt. Soc. Am. B **19**, 1189 (2002).  
[3] A. I. Lvovsky and J. H. Shapiro, Phys. Rev. A **65**, 033830 (2002).  
[4] S. A. Babichev, B. Brezger, and A. I. Lvovsky, Phys. Rev. Lett. **92**, 047903 (2004).

[5] A. Zavatta, S. Viciani, and M. Bellini, Phys. Rev. A **70**, 053821 (2004).  
[6] A. Zavatta, S. Viciani, and M. Bellini, Science **306**, 660 (2004).  
[7] V. Parigi, A. Zavatta, M. S. Kim, and M. Bellini Science **317**, 1890 (2007).  
[8] S. Grandi, A. Zavatta, M. Bellini, M. G. A. Paris, preprint arXiv:1505.03297  
[9] E. Jakeman, C.J. Oliver, and E. R. Pike, Adv. Phys. **24**

- 349 (1975).
- [10] H. P. Yuen, and W. S. Chan, *Opt. Lett.* **8**, 177 (1983).
- [11] B. L. Schumaker, *Opt. Lett.* **9**, 189 (1984).
- [12] G. L. Abbas, V. W. S. Chan, and S. T. Yee, *Opt. Lett.* **8**, 419 (1983).
- [13] B. Yurke, *Phys. Rev. A* **32**, 300 (1985).
- [14] D. T. Smithey, M. Beck, M. G. Raymer, and A. Faridani, *Phys. Rev. Lett.* **70**, 1244 (1993).
- [15] M. G. Raymer, M. Beck, and D. F. McAlister, *Phys. Rev. Lett.* **72**, 1137 (1994).
- [16] D. T. Smithey, M. Beck, J. Cooper, and M. G. Raymer, *Phys. Rev. A* **48**, 3159 (1993).
- [17] K. Vogel and H. Risken, *Phys. Rev. A* **40**, 2847 (1989).
- [18] G. M. D'Ariano, C. Macchiavello, and M. G. A. Paris, *Phys. Rev. A* **50**, 4298 (1994).
- [19] M. Munroe, D. Boggavarapu, M. E. Anderson, and M. G. Raymer, *Phys. Rev. A* **52**, R924 (1995).
- [20] S. Schiller, G. Breitenbach, S. F. Pereira, T. Muller, and J. Mlynek, *Phys. Rev. Lett.* **77**, 2933 (1996).
- [21] G. Breitenbach, S. Schiller, and J. Mlynek, *Nature* **387**, 471 (1997).
- [22] G. M. D'Ariano, M. G. A. Paris, and M. F. Sacchi, *Adv. Imag. Electr. Phys.* **128**, 205-308 (2003).
- [23] A. I. Lvovsky and M. G. Raymer, *Rev. Mod. Phys.* **81**, 299 (2009).
- [24] M. Gu, H. M. Chrzanowski, S. M. Assad, T. Symul, K. Modi, T. C. Ralph, V. Vedral, and P. K. Lam, *Nat. Phys.* **8**, 671 (2012).
- [25] L. S. Madsen, A. Berni, M. Lassen, and U. L. Andersen, *Phys. Rev. Lett.* **109**, 030402 (2012).
- [26] R. Blandino, M. G. Genoni, J. Etesse, M. Barbieri, M. G. A. Paris, P. Grangier, R. Tualle-Broui, *Phys. Rev. Lett.* **109**, 180402 (2012).
- [27] C. Peuntinger, V. Chille, L. Mista, Jr., N. Korolkova, M. Förtsch, J. Korger, C. Marquardt, and G. Leuchs, *Phys. Rev. Lett.* **111**, 230506 (2013).
- [28] V. Chille, N. Quinn, C. Peuntinger, C. Croal, L. Mista, Jr., C. Marquardt, G. Leuchs, and N. Korolkova, *Phys. Rev. A* **91**, 050301(R) (2015).
- [29] F. A. S. Barbosa, A. S. Coelho, K. N. Cassemiro, P. Nussenzveig, C. Fabre, A. S. Villar, and M. Martinelli, *Phys. Rev. A* **88**, 052113 (2013).
- [30] E. H. Huntington, G. N. Milford, C. Robilliard, T. C. Ralph, O. Glöckl, U. L. Andersen, S. Lorenz and G. Leuchs, *Phys. Rev. A* **71**, 041802(R) (2005).
- [31] E. H. Huntington, and T. C. Ralph, *J. Opt. B* **4**, 123 (2002).
- [32] F. A. S. Barbosa, A. S. Coelho, K. N. Cassemiro, P. Nussenzveig, C. Fabre, M. Martinelli, and A. S. Villar, *Phys. Rev. Lett.* **111**, 052113 (2013).
- [33] K. Somiya, *Phys. Rev. D* **67**, 122001 (2003).
- [34] R. W. P. Drever, J. L. Hall, F. V. Kowalski, J. Hough, G. M. Ford, A. J. Munley, and H. Ward, *Appl. Phys. B* **31** 97 (1983).
- [35] H.-A. Bachor, and T. C. Ralph, *A Guide to Experiments in Quantum Optics* (Wiley, 2004).
- [36] S. Olivares, *Eur. Phys. J. Special Topics* **203**, 3 (2012).
- [37] C. Weedbrook, S. Pirandola, R. Garcia-Patrón, N. J. Cerf, T. C. Ralph, J. H. Shapiro, and S. Lloyd, *Rev. Mod. Phys.* **84**, 621 (2012).
- [38] V. D'Auria, A. Porzio, S. Solimeno, S. Olivares, and M. G. A. Paris, *J. Opt. B: Quantum and Semiclass. Opt.* **7**, S750 (2005).
- [39] See the Supplemental material for details about the calculations.
- [40] V. D'Auria, S. Fornaro, A. Porzio, S. Solimeno, S. Olivares, and M. G. A. Paris, *Phys. Rev. Lett.* **102**, 020502 (2009).
- [41] D. Buono, G. Nocerino, V. D'Auria, A. Porzio, S. Olivares, and M. G. A. Paris, *J. Opt. Soc. Am. B* **27**, A110 (2010).
- [42] A. Ferraro, S. Olivares, and M. G. A. Paris, *Gaussian States in Quantum Information* (Bibliopolis, Napoli, 2005).
- [43] R. Simon, *Phys. Rev. Lett.* **84**, 2726 (2000).
- [44] A. Serafini, F. Illuminati, and S. De Siena, *J. Phys. B: At. Mol. Opt. Phys.* **37**, L21 (2004).

## SUPPLEMENTAL MATERIAL

### 1. Covariance matrix elements of the two-mode squeezed thermal state

In this section we explicitly show how we can calculate the elements of the CM  $\sigma'$ , given in Eq. (3) of the main text. We recall that, according to our definitions:

$$b(t, 0|\Omega) = \frac{\hat{a}_{+\Omega}(t) + \hat{a}_{-\Omega}(t)}{\sqrt{2}} \equiv a_s, \quad \text{and} \quad b(t, \pi/2|\Omega) = i \frac{\hat{a}_{+\Omega}(t) - \hat{a}_{-\Omega}(t)}{\sqrt{2}} \equiv a_a, \quad (6)$$

therefore the quadrature operator  $X_\theta(t, \Psi|\Omega) = b(t, \Psi|\Omega) e^{-i\theta} + b^\dagger(t, \Psi|\Omega) e^{i\theta}$  can be written as:

$$X_\theta(t, \Psi|\Omega) = \cos \Psi [q_s \cos \theta + p_s \sin \theta] + \sin \Psi [q_a \cos \theta + p_a \sin \theta]. \quad (7)$$

If we set  $\Psi = 0$ , we have:

$$X_0(t, 0|\Omega) \equiv q_s = a_s + a_s^\dagger = \frac{q_{+\Omega} + q_{-\Omega}}{\sqrt{2}} \Rightarrow \langle q_s^2 \rangle - \langle q_s \rangle^2, \quad (8a)$$

$$X_{\pi/2}(t, 0|\Omega) \equiv p_s = i(a_s^\dagger - a_s) = \frac{p_{+\Omega} + p_{-\Omega}}{\sqrt{2}} \Rightarrow \langle p_s^2 \rangle - \langle p_s \rangle^2, \quad (8b)$$

$$X_{\pm\pi/4}(t, 0|\Omega) \equiv \frac{q_s \pm p_s}{\sqrt{2}} \Rightarrow \frac{1}{2} \langle q_s p_s + p_s q_s \rangle - \langle q_s \rangle \langle p_s \rangle, \quad (8c)$$

for  $\Psi = \pi/2$  we obtain:

$$X_0(t, \pi/2|\Omega) \equiv q_a = a_a + a_a^\dagger = \frac{p_{-\Omega} - p_{+\Omega}}{\sqrt{2}} \Rightarrow \langle q_a^2 \rangle - \langle q_a \rangle^2, \quad (9a)$$

$$X_{\pi/2}(t, \pi/2|\Omega) \equiv p_a = i(a_a^\dagger - a_a) = \frac{q_{+\Omega} - q_{-\Omega}}{\sqrt{2}} \Rightarrow \langle p_a^2 \rangle - \langle p_a \rangle^2, \quad (9b)$$

$$X_{\pm\pi/4}(t, \pi/2|\Omega) \equiv \frac{q_a \pm p_a}{\sqrt{2}} \Rightarrow \frac{1}{2} \langle q_a p_a + p_a q_a \rangle - \langle q_a \rangle \langle p_a \rangle, \quad (9c)$$

On the other hand, if we set  $\Psi = \pm\pi/4$  we find:

$$X_0(t, \pm\pi/4|\Omega) = \frac{q_a \pm q_s}{\sqrt{2}}, \quad \text{and} \quad X_{\pi/2}(t, \pm\pi/4|\Omega) = \frac{p_s \pm p_a}{\sqrt{2}}, \quad (10)$$

ad we have the following identities:

$$\langle X_0^2(t, \pi/4|\Omega) - X_0^2(t, -\pi/4|\Omega) \rangle = 2\langle q_a q_s \rangle \equiv \epsilon_q, \quad (11)$$

$$\langle X_{\pi/2}^2(t, \pi/4|\Omega) - X_{\pi/2}^2(t, -\pi/4|\Omega) \rangle = 2\langle p_a p_s \rangle \equiv \epsilon_p. \quad (12)$$

As mentioned in the main text, it is not possible to calculate the elements  $\delta_{qp}$  and  $\delta_{pq}$  directly from the spectral homodyne traces [1]. However, when the state under consideration is a two-mode squeezed thermal state  $\varrho_\Omega = D_2(\alpha)S_2(\xi)\nu_{+\Omega}(N_1) \otimes \nu_{-\Omega}(N_2)S_2^\dagger(\xi)D_2^\dagger(\alpha)$ , where  $D_2(\alpha) = \exp\{\alpha(a_{+\Omega}^\dagger + a_{-\Omega}^\dagger) - \text{h.c.}\}/\sqrt{2}\}$  is the symmetric displacement operator and  $S_2(\alpha) = \exp(\xi a_{+\Omega}^\dagger a_{-\Omega}^\dagger - \text{h.c.})$  the two mode squeezing operator and  $\nu_{\pm\Omega}(N)$  is the thermal state of mode  $a_{\pm\Omega}$  with  $N$  average photons [2], we can calculate  $\delta_{qp}$  and  $\delta_{pq}$  as follows.

Since the covariance matrix does not depend on the displacement operator, we can assume  $\alpha$ . Furthermore, it is useful to introduce the following parameterization: we define the squeezed photons per mode  $N_{\text{sq}} = \sinh^2 r$ , the total number of thermal photons  $N_{\text{th}} = N_1 + N_2$ , and the thermal-photon fraction  $R_{\text{th}} = N_1/N_{\text{th}}$ . Thereafter, the energies of the two sidebands are given by:

$$N_{+\Omega} = N_{\text{sq}}(1 + N_{\text{th}}) + R_{\text{th}}N_{\text{th}}, \quad (13)$$

$$N_{-\Omega} = N_{\text{sq}}(1 + N_{\text{th}}) + (1 - R_{\text{th}})N_{\text{th}}, \quad (14)$$

respectively, and thus:

$$N_{+\Omega} + N_{-\Omega} = 2N_{\text{sq}} + N_{\text{th}}(1 + 2N_{\text{sq}}) \quad \text{and} \quad N_{+\Omega} - N_{-\Omega} = N_{\text{th}}(2R_{\text{th}} - 1). \quad (15)$$

The covariance matrix associated with  $\varrho_\Omega$  have the following block-matrix form:

$$\sigma_\Omega = \begin{pmatrix} A \mathbb{I} & C \sigma_z \\ C \sigma_z & B \mathbb{I} \end{pmatrix}, \quad (16)$$

where  $\sigma_z$  is the Pauli matrix and:

$$A = 1 + 2N_{\text{sq}}(1 + N_{\text{th}}) + 2R_{\text{th}}N_{\text{sq}}, \quad (17a)$$

$$B = 1 + 2N_{\text{sq}}(1 + N_{\text{th}}) + 2(1 - R_{\text{th}})N_{\text{sq}}, \quad (17b)$$

$$C = 2(1 + N_{\text{th}})\sqrt{N_{\text{sq}}(1 + N_{\text{sq}})}. \quad (17c)$$

The corresponding *measured* covariance matrix reads (see the main text for details):

$$\sigma' = \begin{pmatrix} \frac{1}{2}(A + B) \mathbb{I} + C \sigma_z & (N_{+\Omega} - N_{-\Omega}) i \sigma_y \\ (N_{+\Omega} - N_{-\Omega}) i \sigma_y & \frac{1}{2}(A + B) \mathbb{I} + C \sigma_z \end{pmatrix}, \quad (18)$$

$\sigma_y$  being the Pauli matrix. Note that while  $\sigma'$  is always symmetric,  $\sigma_\Omega$  can be also asymmetric.

## 2. Retrieving the energy unbalance of the two-mode squeezed thermal state

In order to determine the energy *difference* between the sidebands, we should measure the cavity bandwidth and, by exploiting the error signal of the PDH [3], we can assess the relative cavity transmission coefficients  $\tau_{\pm\Omega} = T_{\pm\Omega}/(T_{+\Omega} + T_{-\Omega})$  associated with the two sideband modes, where  $T_{\pm\Omega}$  are the actual transmission coefficients. Therefore, the energy difference can be obtained as:

$$N_{+\Omega} - N_{-\Omega} = \frac{T_{+\Omega} - T_{-\Omega}}{T_{+\Omega} + T_{-\Omega}} (N_{+\Omega} + N_{-\Omega}). \quad (19)$$

In general, given the covariance matrix  $\boldsymbol{\sigma}$  of a Gaussian state, the total energy can be obtained from the sum of its diagonal elements  $[\boldsymbol{\sigma}]_{kk}$  as (without loss of generality we are still assuming the absence of the displacement):

$$N_{\text{tot}} = \frac{1}{4} \sum_{k=1}^4 [\boldsymbol{\sigma}]_{kk} - 1. \quad (20)$$

Experimentally, we can find the total energy  $N_{+\Omega} + N_{-\Omega}$  from the first and second moments of the operators in Eqs. (8) and in Eqs. (9), which are measured from the homodyne detection.

- 
- [1] F. A. S. Barbosa, A. S. Coelho, K. N. Cassemiro, P. Nussenzeig, C. Fabre, A. S. Villar, and M. Martinelli, Phys. Rev. A **88**, 052113 (2013).
  - [2] S. Olivares, Eur. Phys. J. Special Topics **203**, 3 (2012).
  - [3] R. W. P. Drever, J. L. Hall, F. V. Kowalski, J. Hough, G. M. Ford, A. J. Munley, and H. Ward, Appl. Phys. B **31** 97 (1983).